**Proceedings of the ASME-JSME-KSME 2011 Joint Fluids Engineering Conference**
**AJK-Fluids2011**
**July 24-29, 2011, Hamamatsu, Shizuoka, JAPAN**

**AJK2011-09012**

# INFLUENCE OF WATER-SPLASH FORMATION BY A HYDROPHILIC BODY PLUNGING INTO WATER

**Yoshihiro Kubota**
Faculty of Center of Biomedical Engineering Research, Toyo University
Kawagoe, Saitama, Japan

**Osamu Mochizuki**
Faculty of Science and Engineering, Toyo University
Kawagoe, Saitama, Japan

## ABSTRACT

The objective of this study is to understand the relationship between water-splash formation and the surface conditions of bodies plunging into the water's surface by considering hydrophilicity strength. A hydrophilic body (constructed with hydrogel), as well as an acrylic resin body, was created to understand the influence of hydrophilicity on splash formation. The strength of hydrophilicity was determined by investigating degrees of swelling. We obtained consecutive images of splash formation by using a high-speed CMOS camera. We show that water-splash formation is related to water-film formation by studying: 1) droplets formed at the film edge, 2) mushroom- or dome-type splashes caused by film impinging, and 3) crown-type splash caused by film separation. The strength of hydrophilicity affects the splash-formation process of the mushroom- and crown-type splashes. The difference in formation process is caused when the film velocity increases with hydrophilicity. As the film velocity increases with strong hydrophilicity, the film flow separates from the body surface and an air cavity forms. Crown-type splashes form with hydrophilic bodies because such film separation occurs. Moreover, the relationship between the strength of hydrophilicity and film velocity was examined empirically. These results indicate that the hydrophilic body does not alter the splash-formation process.

## INTRODUCTION

This study experimentally investigates the splash formed when a solid body plunges into water focusing on the influence of a hydrophilic body on subsequent splash events.

The body impact on the water surface during a seaplane landing was studied by von Karman (1929) [1], who analyzed the relationship between the gliding angle and landing speed of a seaplane. Do-Quang et al. (2009) numerically studied water splash caused by a spherical body plunging into water [2] and reported a relationship among wetting phenomena, impact velocity, and splash formation. Duez et al. (2007) experimentally reported a relationship between sound generation and splash [3] and observed splash patterns generated by various impact velocities; however, this phenomenon was not discussed in detail. Kubota et al. (2009) studied splash formation by plunging a solid sphere into water [4] and categorized splash patterns according to impact velocity. In addition, they also discussed the characteristics of a film flow generated during the early stage of a splash when a body impacts a water surface.

A droplet colliding with a solid surface also generates a water splash. Yoon et al. (2007) studied film-like structures and their instability [5]. Bejan et al. (2006) and Bussmann et al. (2000) reported the deformation of a droplet colliding with a solid surface numerically and experimentally [6,7]. The appearance of numerous finger-like structures at the edge of a spreading film was discussed according to the Rayleigh–Taylor instability theory [4]. Kubota et al. (2009) showed that instability is relative to the number of droplets generated from an edge of a film flow [4] and that droplets are generated by a primary splash appearing at the first stage of a sphere's impact on the water surface. Worthington (1882) investigated the milk crown for droplet-liquid collision and the splash caused by a solid body falling into a liquid [8]. Akers et al. (2006) studied the splash of a non-Newtonian fluid [9] and showed that the deformation of an air cavity is caused by various fluid properties. Truscott et al. (2006) investigated the splash formed by a spinning, spherical body plunging into water [10] focusing on underwater air cavity formation.

In this study, hydrophilicity of a body surface was determined using a hydrogel, which is currently employed for flow control in laminar flows. Eddington et al. (2003) reported the use of hydrogel as a valve for flow control on microchannels [11], and Beebe et al. (2000) reported the

effectiveness of hydrogel structures for flow control on microfluidic channels.

Although the splash phenomenon is familiar, the detailed mechanism of its formation is not well understood. To understand the influence of hydrophilic bodies on splashes, we performed experiments with two solid bodies composed of different materials—acrylic resin and hydrogel—and we determined that these materials result in a distinctive affinity of body and water. The splash formation was observed using a high-speed CMOS camera to capture consecutive images. In this paper, we use the film-formation process to explain the effects of surface conditions on splash formation. In addition, we discuss the effects of hydrophilicity on splash formation and the velocity of film flow as the body plunges into water.

## EXPERIMENTAL SETUP

To study splash formation, we observed a solid body plunging into water in a 300 × 300 × 400 $mm^3$ tank filled with tap water up to 340 mm. Our previous experiment (Kubota et al. 2009) confirmed that tap-water contaminants do not affect splash formation [4]. Consecutive images of the splash-formation process were recorded from the side of the water tank by using a high-speed CMOS camera (Vision Research Inc., Phantom v7.1) set at 4000 frames per second (fps). The timing precision of consecutive frames was 0.25 ms. A 500-W halogen lamp was used as volumetric illumination.

Spherical models were produced from an acrylic resin and hydrogel with diameters ($D = 2r$) of 20 mm. Hydrogel was used as agar gel in our experiment. The wetness of the models was varied to understand the influence of hydrophilicity strength on the body. The wetness was determined by the amount of water in the models as a degree of swelling; it is described as the relationship between the mass of hydrogel and total mass of water and hydrogel, represented by $s = (m_{gel} + m_{water})/m_{gel}$. Here $s$ is the degree of swelling, $m_{gel}$ is the mass of gel, and $m_{water}$ is the mass of water. The degree of swelling was considered with $s$ = 0, 50, 100, and 150; $s$ = 0 implies that water was not contained inside the model as in the case of the acrylic model.

We carefully wiped the body surfaces with paper towels to remove stains such as oil and to ensure uniform surface conditions before each trial. The impact velocity $V_i$ of the model at the water surface was varied by changing the initial height $h$, where $h$ was measured from the water surface to the bottom of the model. $h$ was varied from 1$D$ to 45$D$, which resulted in a $V_i$ range from 0.63 to 5.6 m/s. $V_i$ was calculated by $V_i = (2gh)^{0.5}$ based on energy conservation. Because $h$ was small, air drag was neglected in this calculation. A launcher system held each model via suction at $h$ just before release, and all models plunged into the water surface without rotation or horizontal displacement. Hence, all experiments were reproducible.

Figure 1 shows a tree diagram of splash patterns at various time intervals; splash is represented by shadowed regions in the figure. The three types of splashes are primary, secondary, and tertiary, and their progress depends on $V_i$. The primary splash initially appeared as a film flow when the body touched the water surface, and tiny droplets were generated from the edge of this film flow. The number of droplets was determined on the basis of the instability theory related to the film edge. The droplets flew out in a direction tangential to the position from which they detached. The secondary splash was a result of the primary splash. If the film flow ran along the wall of the sphere, the edge of the film merged at the rear center of the model, and the secondary splash assumed the form of a mushroom-type splash. If the separated film flow converged behind the model, the secondary splash took the form of a dome-type splash. If the film flow did not close at the rear of the model, no secondary splash appeared. The tertiary splash developed by a reaction of the air cavity when the body quickly entered the water; if an air cavity did not form, the tertiary splash did not appear. The air cavity is related to the detachment of the film flow from the body surface. Thus, the behavior of the primary splash strongly affected all subsequent splash-formation processes.

Kubota et al. (2010) showed the influence of a tail shape on the formation of subsequent splash events [13] and reported the relationship between the body shape and film meet [Remark 6] for splash formation. They studied the relationship between tail shape and secondary-splash formation and discussed the effect of tail shape on secondary-splash volume and formation time. Kubota et al. (2010) investigated the influence of head shape on the formation of subsequent splash events [14], focusing on film formation relative to head shape differences. The film thickness was determined by investigating the momentum relationship between the body and the film.

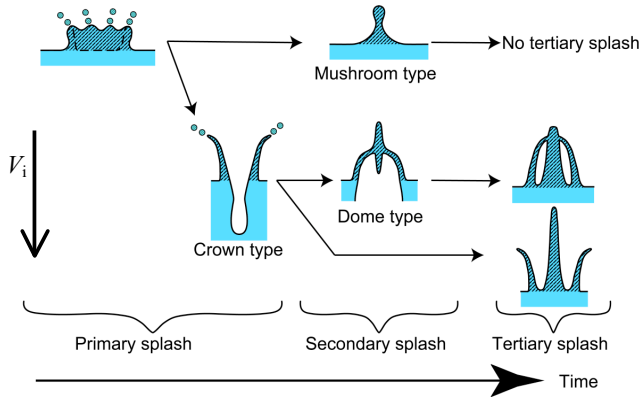


**FIGURE 1.** TREE DIAGRAM SHOWING SPLASH FORMATION PROCESSES FOR VARIOUS IMPACT VELOCITIES $V_i$ AND BODY SHAPES.

## EXPERIMENTAL RESULTS

Three dimensionless parameters were used to understand splash formation: time, Reynolds number, and Weber number. Dimensionless time $T$ is defined as $T = tV_i/D$, where $t$ is the measured time. This variable is useful for comparing splash-formation processes for different conditions of $V_i$. Even if $V_i$ varies, $T = 1$ indicates the same dimensionless time intervals during which the model moves by a distance equal to the diameter $D$. $T = 0$ indicates the moment at which the head of the model touches the water surface. Reynolds number $Re$ and Weber number $We$ are useful for understanding the relationship between the kinetics of the body and fluid characteristics. $Re = V_i D/v$, where $v$ is the kinematic viscosity of water at 25 °C, and $We = \rho V_i^2 D/\sigma$, where $\rho$ is the density and $\sigma$ is the surface tension of water at 25 °C. These dimensionless parameters were calculated using body diameter $D$ and impact speed $V_i$.

### Splash-Formation Process

The splash-formation process by an acrylic sphere is shown in Fig. 2. The sequence of splash formation and the timing is expressed by $T$ as previously defined. The conditions in this experiment were $V_i = 3.1$ m/s, $We = 2.6 \times 10^3$, and $Re = 7.1 \times 10^4$. In the initial stage of splash formation until $T = 0.12$, the film flow formed immediately after the body impacted the water surface. A tiny droplet of primary splash that formed from the finger-like structure at the edge of the film was related to film-edge instability. Thus, the number of formed droplets was examined analytically and expressed by the Rayleigh–Taylor instability [4]. When $T = 0.25$, the film flow moved along the body surface, and droplets were generated continuously from the edge of film. Later, the film meet occurred when the film flow covered the body at $T = 0.72$, generating a secondary splash known as a mushroom-type splash. This occurrence indicates that the secondary splash cannot form in the absence of film converging. If film separation occurred, an air cavity formed that caused a tertiary splash (Fig. 1).

We next focused on the relationship between body wetness and film flow caused by the body's impact with the water surface. Because all splash formations such as primary droplets, secondary mushroom types, and tertiary splashes are associated with film formation [4,5], the details of splash formation by the influence of hydrophilic bodies are discussed below.

### Relation between splash formation and body surface conditions

Hydrophilic body strength was determined by degrees of swelling (*s)* as previously defined. Figure 3 shows a comparison of splash formation and body wetness. These results were obtained at $T = 2.0$. The result by an acrylic body is shown by $s = 0$ because the inside of the body does not contain water. The results by hydrogel are shown as $s = 50$ and $s = 100$. All results exhibited film formation when the body impacted the water surface, and droplets were generated from the edge of the film. The result in $s = 0$ showed a mushroom-type splash caused by the convergence of the films over the model that was formed when the air cavity under the water was nonexistent. The results of the hydrogel model on $s = 50$ and $s = 100$ were observed as dome-type splashes that formed when the body was under water before being covered by the film. The air-cavity depth changed with the difference in the degree of swelling between $s = 50$ and $s = 100$, increasing with the

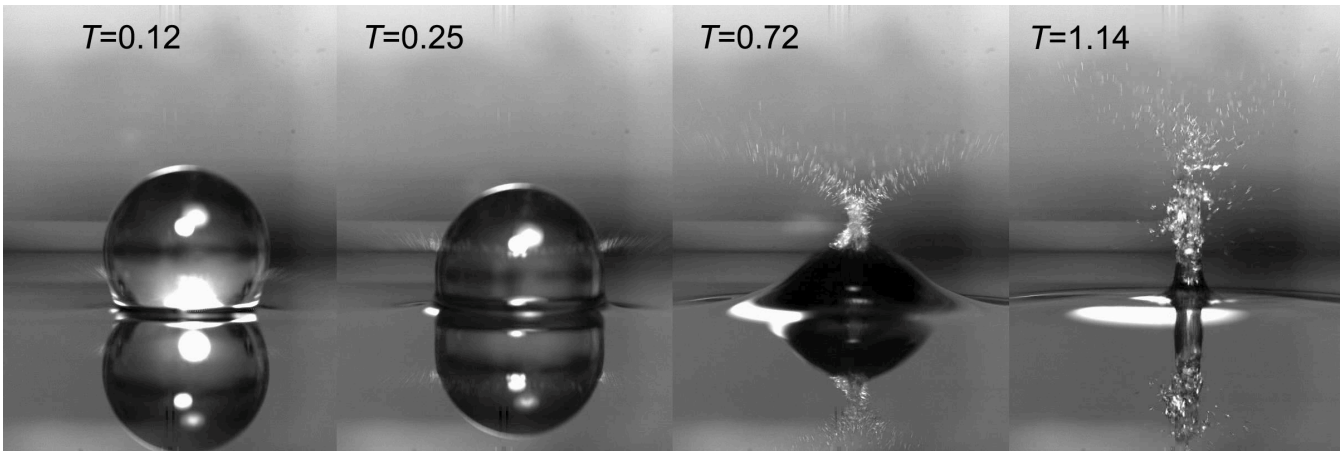


**FIGURE 2.** SEQUENCE OF SPLASH FORMATION AT $V_i = 3.1$m/s.

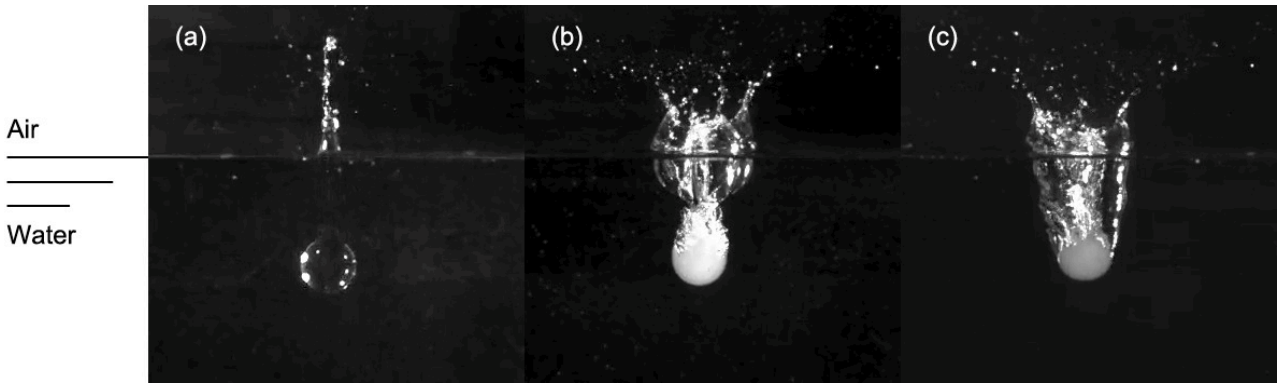


**FIGURE 3.** COMPARISON OF SPLASH FORMATION AT $V_I = 3.1$ M/S. (A) $S = 0$ (ACRYLIC MODEL), (B) $S = 50$, AND (C) $S = 100$.

strength of hydrophilicity. This result suggests that the hydrophilic body strength affects film-flow velocity. The film velocity was measured to understand the relationship between the film velocity and the degree of body swelling.

Figure 4 shows the maximum film velocity $V_{fmax}$ measured at $T = 0.05$ for different $V_i$. The results of $s = 0$ are shown as a relationship between $V_{fmax}$ and $V_i$. $V_{fmax}$ by $s = 50$ and $s = 100$ was measured at $V_i = 3.1$ m/s for comparison. From the result of $s = 0$, $V_{fmax}$ is proportional to $V_{fmax} = 8.3V_i$. The film velocity was measured by an image analysis. This comparison shows that the film velocity on a hydrophilic body was more than twice the speed of $s = 0$ in the case of an acrylic body. This film velocity increase caused the film to separate from the body surface [4], which is explained by the force balance between the centrifugal force acting on the film and the film's surface tension [4, 13]. If the centrifugal force was greater than the surface tension, the film separated from the body surface. Film velocity increased with the degrees of swelling on the body; thus, the hydrophilicity of the body is related to splash formation, and thus, it is necessary to understand the relationship between hydrophilicity strength and splash formation.

The relationship between film velocity and degree of swelling as hydrophilicity is shown in Fig. 5. The red circle shows the experimental result, and the blue solid line shows the empirical result with a logarithmic function as $V_{fmax} = 0.98\ln(s)$. The empirical result shows the evidence of higher film velocity with an increase in body hydrophilicity as illustrated in Fig. 3. Comparison of the cavity depth with the strength of degrees of swelling in the flow visualization indicates that strong hydrophilicity creates a deep air cavity. This result implies that the air-cavity formation needs to be considered as potential energy of the model for impact velocity and also for film

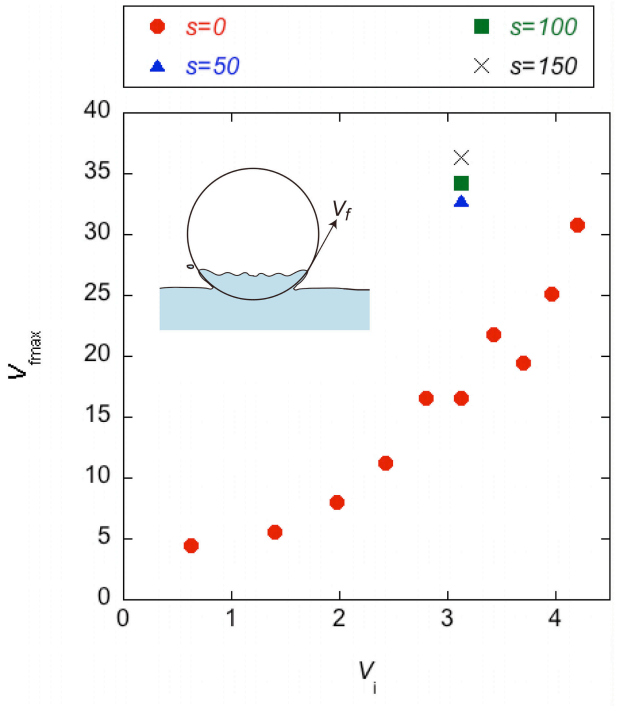


**FIGURE 4.** VELOCITY ($V_{fmax}$) OF FILM-FLOW MEASURED AT $T = 0.05$ FOR DIFFERENT $V_i$.

velocity. Thus, the combination of impact velocity and film velocity affects tertiary-splash formation because tertiary splash is formed by air-cavity reaction. In addition, the empirical line shows good agreement with the experimental value; therefore, the film velocity on a hydrophilic body can be examined by a logarithmic function.

When $V_i < 0.9$ m/s, a spire-type splash formed through a reaction of water-surface concavity [4]. From the relationship between film velocity and impact velocity, increasing velocity of the film with impact velocity indicates that the film velocity at low impact also increases. Therefore, the threshold impact velocity between spire-type and mushroom-type splashes ($V_i <$ 0.9 m/s as $s = 0$) changes with a hydrophilic body. The splash formation was visualized to confirm the increase in film velocity (Fig. 6). Figure 6(a) shows the formation of a spire-type splash with $s = 0$, and Fig. 6(b) shows the result at $s = 50$. The spire-type splash in Fig. 6(a) was formed by a concavity reaction. This type of splash cannot be observed in Fig. 6(b) because the film flow covered the body before the concavity formed. This finding also indicates the importance of understanding the relationship between film velocity and body impact velocity.

## CONCLUDING REMARKS

The influence of hydrophilic bodies on splash formation caused by a body's impact with the water surface was demonstrated using a high-speed CMOS camera. Hydrogel was used to consider hydrophilicity, the strength of which varied with the degrees of swelling. Four degrees of swelling were investigated: $s = 0$, 50, 100, and 150. The degree of swelling showed the amount of water inside the model; the result of the acrylic model showed $s = 0$. Varying the body status determined the influence relation between film flow and surface conditions.

The converging of films with hydrophilicity caused a change in the splash-formation process of a secondary splash. For an acrylic body, $s = 0$, a mushroom-type splash formed, and a dome-type splash appeared at $s = 50$ and $s = 100$. Film-flow separation from the body surface, caused by an increase in film velocity, created the difference in splash types and was related to air-cavity formation, which was in turn related to tertiary-splash formation. The hydrogel model generated additional splashes as tertiary splashes. The increase in film velocity with the degree of swelling of body was obtained empirically. The film velocity was changed logarithmically. Thus, the influence of hydrophilicity on splash formation affects film velocity, and a change in the film velocity causes film separation and the formation of tertiary splashes.

## NOMENCLATURE

$s$ Degree of swelling defined as $s = (m_{gel} + m_{water})/m_{gel}$.
$m_{gel}$ Mass of gel.
$m_{water}$ Mass of water inside the model.
$V_i$ Impact velocity of body.
$g$ Gravitational acceleration.

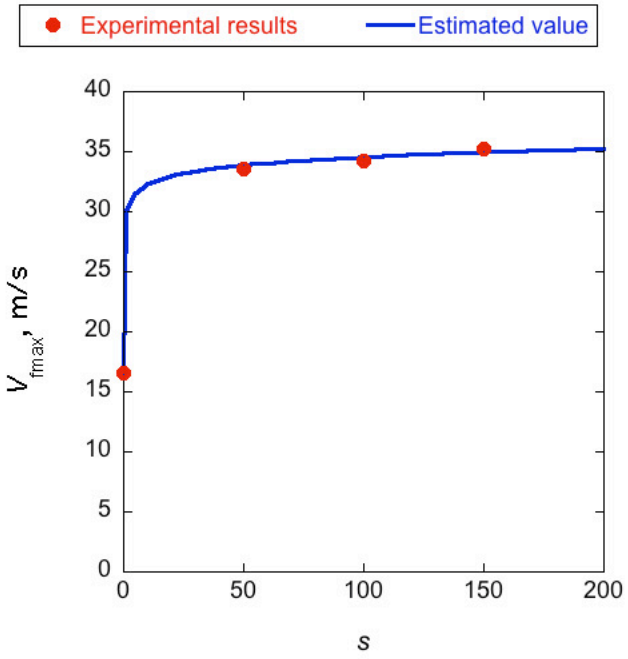


**FIGURE 5.** VELOCITY ($V_{fmax}$) OF FILM FLOW MEASURED AT $T = 0.05$ S FOR DIFFERENT BODY WETNESS.

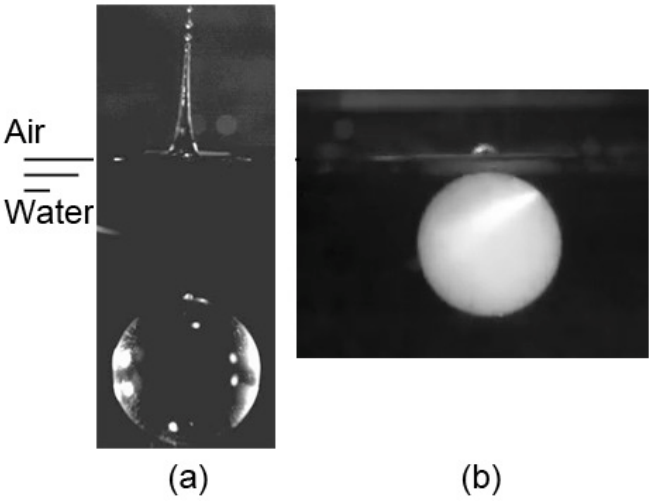


**FIGURE 6.** COMPARISON OF SPLASH FORMATION AT $V_i =$ 0.63 M/S. (A) $S = 0$ (ACRYLIC MODEL) AND (B) $S = 50$.

$h$ Initial height of body.
$T$ Dimensionless time defined as $T = tV_i/D$.
$t$ Measured time.
$Re$ Reynolds number defined as $Re = V_i D/v$
$v$ Kinematic viscosity of water at 25 °C
$We$ Weber number defined as $We = \rho V_i^2 D/\sigma$
$\rho$ Density of water at 25 °C.
$\sigma$ Surface tension of water at 25 °C.
$V_{fmax}$ Measured maximum film velocity.

## REFERENCES


[1] von Karman 1929. "The impact on seaplane floats during landing" *National Advisory Committee for Aeronautics Technical* **Note 321**.

[2] Do-Quang, M, and Amberg, G (2009). "The splash of a solid sphere impacting on a liquid surface: Numerical simulation of the influence of wetting" *Physics of Fluid*, **21**, pp 022102-1-022102-13.

[3] Duez, C, Y, Clanet, C, and Bocquet, L (2007). "Making a splash with water repellency" *Nature Physics*, **3,** pp 180-183.

[4] Kubota, Y, and Mochizuki, O (2009). "Splash Formation by a Spherical Body Plunging into Water" *Journal of Visualization*, **12**, pp 339-345.

[5] Yoon, S, S, Jepsen, R, A, Nissen, M, R, and O'Hern, T, J (2007) "Experimental investigation on splashing and nonlinear fingerlike instability of large water drops" *Journal of Fluids and Structure*, **23**, pp 101-115.

[6] Bejan, A, and Gobin, D (2006). "Constructal theory of droplet impact theory" *International Journal of Heat and Mass Transfer*, **49**, pp 2412-2419.

[7] Bussmann, M, Chandra, S, and Mostaghimi, J (2000) "Modeling the splash of a droplet impacting a solid surface" *Physics of Fluids*, **12**, pp 3121-3132.

[8] Worthington, A, M, (1882-1883). "On Impact with a Liquid Surface" *Proceedings of the Royal Society of London*, **34**, pp 217-230.

[9] Akers, B, and Belmote, A (2006). "Impact dynamics of a solid sphere falling into a viscoelastic micellar fluid" *Journal of Non-Newtonian Fluid Mechanics*, **135**, pp 97-108.

[10] Truscott, T, T, and Techt, A, H (2006) "Cavity formation in the wake of spinning of sphere impacting the free surface" *Physic of Fluids*, **18**, pp 091113-1.

[11] Beebe, D, J, Moore, J, S, Bauer, J, M, Yu, Q, Liu, R, H, Devadoss, C, Jo, B-H (2000). "Functional hydrogel structures for autonomous flow control inside microfluidic channels" *Nature*, **404**(6778), pp 588-590.

[12] Eddington, D, T. and Beebe, D, J (2004). "Flow control with hydrogels" *Advanced Drug Delivery Reviews*, **56**(2), pp 199-210.

[13] Kubota, Y, and Mochizuki, O (2010). "ELEMENTAL STRUCTURE OF SPLASH GENERATED BY A PLUNGING SOLID BODY" *Journal of Flow Visualization and Image Processing*, 17(4), pp 359-369.

[14] Kubota, Y., and Mochizuki, O (2009). "Influence of head shape of solid body plunging into water on splash formation" *Journal of Visualization*, in printing.